J. Plasma Physics (1997), *vol.* 58, *part* 2, *pp.* 205–221. Printed in the United Kingdom
© 1997 Cambridge University Press

Linear mode analysis in multi-ion plasmas

G. MANN,[1] P. HACKENBERG[1] and E. MARSCH[2]

[1]Astrophysikalisches Institut Potsdam, Telegrafenberg A31, D-14473 Potsdam, Germany

[2]Max-Planck-Institut für Aeronomie, Postfach 20, D-37191 Katlenburg–Lindau, Germany

(Received 29 January 1996 and in revised form 27 January 1997)

Heavy ions frequently appear as minor components in space plasmas, for example in the solar wind and in the vicinity of comets. Both the different components of ions and the associated plasma waves are observed by extraterrestrial *in situ* measurements. The influence of these ion components on the properties of plasma waves is investigated by means of the multi-fluid equations. The linear mode analysis is performed numerically for a three-component plasma with an ambient magnetic field. Both the dispersion relations and the polarizations of the freely propagating wave modes are given and subsequently discussed.

1. Introduction

Plasmas with several kinds of particle species and/or populations appear in different regions of the heliosphere. Two general cases can be distinguished. In the first the plasma consists of different species, i.e. electrons, protons and heavy ions. This situation is found in the fully ionized solar wind with helium ions and many minor heavy ions, or in the plasma of pick-up heavy ions in the vicinity of comets. The cometary matter escaping as a neutral gas from the nucleus of the comet is ionized by various processes, such as photo-ionization (Thomsen *et al.* 1987). Thus ionized oxygen and/or water-group ions exist in the vicinity of comets. Secondly, one sort of ion may appear in populations with different properties, for example a thermal and a hot streaming component of protons. This situation is often found in highly non-thermal plasmas, such as boundary layers, (e.g. interplanetary shocks, planetary bow shocks, or corotating interaction regions in the solar wind). At these boundaries, a small part of the thermal ions, i.e. protons and heavy ions, are heated and/or accelerated (for a review see e.g. Thomsen 1985). In both cases large-amplitude low-frequency magnetic field fluctuations are observed by extraterrestrial *in situ* measurements at the Earth's bow shock (Paschmann *et al.* 1979; Hoppe *et al.* 1981; Mann and Lühr 1991), at other planetary bow shocks (Fairfield and Behannon 1976; Hoppe and Russell 1981; Goldstein *et al.* 1983), and in the vicinity of comets Giacobini–Zinner (Tsurutani and Smith 1986; Tsurutani *et al.* 1987*a*) and Halley (Riedler *et al.* 1986; Tsurutani *et al.* 1987*b*).

Many of the observed low-frequency magnetic field fluctuations appear only in association with a special ion component (e.g. heavy ions, hot protons, and proton streams) besides the background electrons and protons. These low-frequency magnetic field fluctuations reveal low-frequency plasma waves in space plasmas. Here, 'low frequency' means frequencies essentially lower than the electron plasma

https://doi.org/10.1017/S0022377897005758 Published online by Cambridge University Press

frequency ω_{pe} and the electron cyclotron frequency ω_{ce}. Thus these waves are predominantly carried by the ions, and the electrons act only as a neutralizing fluid.

The properties of these low-frequency plasma waves can be studied very well by evaluating extraterrestrial magnetic field measurements. Motivated by these observations, a comprehensive linear mode analysis of a multi-ion plasma is presented in this paper. Of course, this has already been partly done in the context of different (but special) problems, for instance by Smith and Brice (1964), Hamelin and Beghin (1976), Verheest (1977), Rönnmark (1982), Isenberg and Hollweg (1982), Isenberg (1984), Melrose (1986), Oscarson and Andre (1986), Hizanidis *et al.* (1988), Zank and McKenzie (1988), Temerin and Roth (1992), McKenzie *et al.* (1993) and Miller and Viñas (1993).

Here we intend to present a complete study of these waves by means of the multi-fluid equations supplemented by Maxwell's equations and the equations of state of each particle component in a magnetized plasma. Going beyond previous investigations, the dispersion relations $\omega = \omega(\mathbf{k})$, the group velocity $\mathbf{v}_g = \mathbf{v}_g(\mathbf{k}) = \nabla_{\mathbf{k}}\,\omega(\mathbf{k})$ and the angles $\psi = \psi(\mathbf{k})$ between the direction of the group velocity and the ambient magnetic field are derived for the plasma waves considered. Here ω and $\mathbf{k}$ denote the frequency and wavenumber of the waves. Wave propagation directions parallel, perpendicular and oblique (e.g. 30°) to the ambient (constant) magnetic field are considered. Furthermore, the degree of circular polarization (helicity) $\sigma(\mathbf{k})$ and the electrostatic part $\xi(\mathbf{k})$ of these waves are studied.

In Sec. 2 the multi-fluid equations supplemented by Maxwell's equations are presented and subsequently linearized. The linear mode analysis results in a complex dispersion relation. The results are discussed in much detail for a cold and warm bi-ion plasma in Sec. 3.

2. Basic equations

We shall treat the collisionless multi-ion plasma by means of multi-fluid equations (see Krall and Trivelpiece 1973). Each plasma component is denoted by a label α, and is characterized by the particle number density N_α, the streaming velocity $\mathbf{v}_\alpha$, the particle mass m_α, the particle charge q_α and the isotropic partial pressure p_α. Then the equation of continuity and the momentum equation of each particle component can be written as

$$\frac{\partial}{\partial t} N_\alpha + \nabla \cdot (N_\alpha \mathbf{v}_\alpha) = 0 \tag{2.1}$$

$$\frac{\partial}{\partial t} \mathbf{v}_\alpha + (\mathbf{v}_\alpha \cdot \nabla)\, \mathbf{v}_\alpha + \frac{1}{m_\alpha N_\alpha} \nabla p_\alpha - \frac{q_\alpha}{m_\alpha} \left(\mathbf{E} + \frac{\mathbf{v}_\alpha \times \mathbf{B}}{c} \right) = 0 \tag{2.2}$$

The behaviour of the electric field $\mathbf{E}$ and magnetic field $\mathbf{B}$ are prescribed by Maxwell's equations:

$$\nabla \times \mathbf{E} = -\frac{1}{c} \frac{\partial}{\partial t} \mathbf{B}, \tag{2.3}$$

$$\nabla \times \mathbf{B} = \frac{1}{c} \frac{\partial}{\partial t} \mathbf{E} + \frac{4\pi}{c} \mathbf{j}, \tag{2.4}$$

$$\nabla \cdot \mathbf{E} = 4\pi\rho, \tag{2.5}$$

$$\nabla \cdot \mathbf{B} = 0, \tag{2.6}$$

https://doi.org/10.1017/S0022377897005758 Published online by Cambridge University Press

where, c is the velocity of light. The charge density ρ and the current density $\mathbf{j}$ are given by

$$\rho = \sum_{\alpha} q_\alpha N_\alpha, \tag{2.7}$$

$$\mathbf{j} = \sum_{\alpha} q_\alpha N_\alpha \mathbf{v}_\alpha \ . \tag{2.8}$$

This set of equations is closed by making the assumption of a polytropic equation of state for each particle component:

$$p_\alpha = p_{0\alpha} \left(\frac{N_\alpha}{N_{0\alpha}} \right)^{\gamma_\alpha} \ . \tag{2.9}$$

Here $p_{0\alpha}$ and $N_{0\alpha}$ are the unperturbed or background values of the partial pressures and the particle number densities, which would be present if there were no waves. We shall always use subscript 0 if we are referring to an unperturbed quantity.

The unperturbed magnetic field is parallel to the unit vector $\mathbf{e}_B$, i.e. $\mathbf{B}_0 = B_0 \, \mathbf{e}_B$. All plasma components are moving along this direction with speeds $v_{0\alpha}$ in the undisturbed case. There is no background electric field. Charge neutrality and a current-free state are assumed to exist in the unperturbed plasma, i.e. $\rho_0 = \sum_\alpha q_\alpha N_{0\alpha} = 0$ and $\mathbf{j}_0 = \sum_\alpha q_\alpha N_{0\alpha} v_{0\alpha} \mathbf{e}_B = 0$.

The subsequent tedious but straightforward process of normalization and linearization is done in the appendix. Among other things, frequencies are normalized to the proton cyclotron frequency, and wavenumbers are related to a length of reference l_{ref} as introduced in the appendix.

Since we are interested in the study of plane waves, the wave vector is assumed to be directed along the x axis, i.e. $\mathbf{k} = k \, \mathbf{e}_x$, and the ambient magnetic field lies in the (x, z) plane, i.e. $\mathbf{e}_B = \cos\theta \, \mathbf{e}_x + \sin\theta \, \mathbf{e}_z$. As demonstrated in the appendix, the linearization of the basic equations (2.1)–(2.9) and their subsequent Fourier transformation result in an algebraic equation of the form

$$[n^2 \, (\mathbf{e}_x \otimes \mathbf{e}_x - \mathbf{1}) + \boldsymbol{\epsilon}] \, \mathbf{E} = 0, \tag{2.10}$$

with the refractive index $n = ck/\omega$ and the dielectric tensor

$$\boldsymbol{\epsilon} = \begin{pmatrix} \epsilon_1 & i\epsilon_6 & \epsilon_5 \\ -i\epsilon_6 & \epsilon_2 & i\epsilon_4 \\ \epsilon_5 & -i\epsilon_4 & \epsilon_3 \end{pmatrix} \ . \tag{2.11}$$

Here $\otimes$ denotes the dyadic product.

Solutions of (2.10) have the following form

$$\mathbf{E} = A \, (p_1 \mathbf{e}_x + i p_2 \mathbf{e}_y + p_3 \mathbf{e}_z) \, \mathrm{e}^{i(kx - \omega t)}, \tag{2.12}$$

with $p_1^2 + p_2^2 + p_3^2 = 1$. Thus p_1, p_2 and p_3 are real numbers that characterize the polarization unambiguously. This is only true for real ω and k. Note that ω becomes a complex number in the case of instabilities. Non-trivial solutions (i.e. A is not zero) can be found only if

$$\det[n^2 \, (\mathbf{e}_x \otimes \mathbf{e}_x - \mathbf{1}) + \boldsymbol{\epsilon}] = 0 \ . \tag{2.13}$$

The evaluation of the determinant leads to a polynomial in ω and k of usually high order. Therefore the polynomial's roots can be found analytically only in very special and simplified cases. A polynomial of order P in ω leads to P different

https://doi.org/10.1017/S0022377897005758 Published online by Cambridge University Press

solutions $\omega_\delta(k)$ ($\delta = 1, \ldots, P$). These solutions are the dispersion relations of the different plasma waves. The phase and group velocity are, as usual, defined by $v_{\rm ph} = \omega/k$ and $\mathbf{v}_{\rm g} = \nabla_{\mathbf{k}}\,\omega$ respectively. The group velocity lies in the plane of $\mathbf{k}$ and $\mathbf{B}_0$, i.e. the (x,z) plane. The absolute value and the direction of the group velocity are given by

$$v_{\rm g} = \left[\left(\frac{\partial\omega}{\partial k}\right)^2 + \frac{1}{k^2}\left(\frac{\partial\omega}{\partial\theta}\right)^2\right]^{1/2}, \tag{2.14}$$

$$\psi = \arctan\left[\left(\frac{\partial\omega}{\partial k}\sin\theta + \frac{1}{k}\frac{\partial\omega}{\partial\theta}\cos\theta\right)\Big/\left(\frac{\partial\omega}{\partial k}\cos\theta - \frac{1}{k}\frac{\partial\omega}{\partial\theta}\sin\theta\right)\right]. \tag{2.15}$$

The propagation angle ψ is measured from $\mathbf{B}_0$ in the direction of $\mathbf{k}$, i.e. $\mathbf{v}_{\rm g}$ parallel to $\mathbf{B}_0$ would result in $\psi = 0$ and $\mathbf{v}_{\rm g}$ parallel to $\mathbf{k}$ would result in $\psi = \theta$.

We shall now examine the types of polarization that (2.12) allows. In order to do this, we set the amplitude A equal to unity and look at the real part of the electric field. The phase offset contained in A and the argument of the exponentional function are simply denoted by ϕ. Thus we obtain

$$\mathrm{Re}\,\mathbf{E} = (p_1\mathbf{e}_x + p_3\mathbf{e}_z)\cos\phi - p_2\mathbf{e}_y\sin\phi \tag{2.16}$$

from (2.12) for $|A| = 1$. This is a parametric form of an ellipse with one principal axis parallel to $\mathbf{e}_y$. The other principal axis is located in the (x,z) plane. We can also characterize this ellipse by the length of the principal half axes, $|p_2|$ and $(p_1^2+p_3^2)^{1/2}$, and by the angle $\gamma = \arctan(p_1/p_3)$ at which the plane of the ellipse is tilted with respect ω the (y,z) plane. A negative sense of revolution may be denoted by $\gamma \in (\frac{1}{2}\pi, \frac{3}{2}\pi)$.

Another (but equivalent) approach is the decomposition into orthogonal polarization modes:

$$\mathbf{E} = A\left[S\mathbf{e}_x + R\sqrt{\tfrac{1}{2}}(-i\mathbf{e}_y + \mathbf{e}_z) + L\sqrt{\tfrac{1}{2}}(\mathrm{i}\mathbf{e}_y + \mathbf{e}_z)\right]\,\mathrm{e}^{i(kx-\omega t)}\,. \tag{2.17}$$

The three parameters S, R and L are real and are normalized to unity ($S^2+R^2+L^2 = 1$). They represent the magnitudes of the longitudinal or sonic, and the right-hand circular and left-hand circular components of the wave, respectively. Then it is more convenient to define the helicity (see e.g. Krauss-Varban *et al.* 1994) by

$$\sigma = \frac{R^2 - L^2}{R^2 + L^2} = -2\,\frac{p_2 p_3}{p_2^2 + p_3^2}\,. \tag{2.18}$$

Here transverse right-hand, left-hand circular polarization and linear polarization correspond to $\sigma = 1$, -1 and 0 respectively. Furthermore,

$$\xi = S\frac{R+L}{|R+L|} = p_1\frac{p_3}{|p_3|} \tag{2.19}$$

denotes the longitudinal contribution to the wave. In the case of fully transverse polarization, $\xi = 0$.

Negative ξ indicates that p_1 and p_3 have different signs. Thus a zero-crossing of $p_3(k)$ influences the graph of $\xi(k)$. Zero-crossings of p_3 are always connected with $\sigma = 0$. Note, that also $p_2 = 0$ leads to $\sigma = 0$. This effect can be seen on the dotted line for ξ at $k \approx 0.5$ in Fig. 3. There both p_1 and p_3 change signs simultaneously. The other case, where only p_3 changes its sign, can be seen in Fig. 5 at $k \approx 0.502$

https://doi.org/10.1017/S0022377897005758 Published online by Cambridge University Press

($|\xi| \approx 0.08$, dotted line) and $k \approx 1.16$ ($|\xi| \approx 0.982$, dashed line). Both functions $\xi(k)$ have a jump due to the change in sign of p_3.

3. Mode analysis

We shall now discuss the dispersion relations and polarizations of the different plasma waves in a more detailed fashion. As mentioned above, the dispersion relation is given implicitly by (2.13). This equation can generally be written as a polynomial in ω and k:

$$P(\omega, k) = \sum_{p,q=0}^{P,Q} a_{p,q}\, \omega^p\, k^q = 0 \tag{3.1}$$

First, we search for the cut-off frequencies, which are defined by $\omega_{\mathrm{cut}\,\delta} = \omega_\delta(k{=}0)$. The case $\omega_{\mathrm{cut}\,\delta} > 0$, leads to the requirement that the refractive index become zero, i.e. $n = 0$. Then the determinant of the dielectric tensor $\boldsymbol{\epsilon}$ is zero (see (2.13)). This condition is independent of the bulk velocities $v_{0\alpha}$, the plasma betas β_α and the wave propagation angle θ. Consequently, the cut-off frequencies do not depend on these parameters.

In order to study the influence of the minor ion components on the properties of plasma waves with respect to dispersion and polarization, we restrict ourselves to a bi-ion plasma, i.e. the plasma consists of electrons, protons and a minor ion component of a charge Ze and mass Mm_p. The relative abundance of ions is given by ν via $N_{0i} = \nu N_{0e}$. To ensure charge neutrality of the undisturbed plasma, the proton density must be set to $N_{0p} = (1 - Z\nu) N_{0e}$. Because of the normalization used above, our equations depend only on the parameters Z, M and ν. Thus we find four such cut-off frequencies. Three of them are located in the vicinity of the electron plasma frequency, namely,

$$\omega_{\mathrm{cut}\,1} = \omega_p = \left(\sum_\alpha \omega_{p\alpha}^2 \right)^{1/2} \approx \omega_{pe}\ . \tag{3.2}$$

$$\omega_{\mathrm{cut}\,2} = \omega_R \approx \omega_{pe} \left(1 + \frac{\omega_{ce}^2}{4\,\omega_{pe}^2} \right)^{1/2} + \frac{\omega_{ce}}{2}, \tag{3.3}$$

$$\omega_{\mathrm{cut}\,3} = \omega_L \approx \omega_{pe} \left(1 + \frac{\omega_{ce}^2}{4\,\omega_{pe}^2} \right)^{1/2} - \frac{\omega_{ce}}{2} \tag{3.4}$$

(see Krall and Trivelpiece 1973). The fourth is of the order of the ion cyclotron frequency:

$$\omega_{\mathrm{cut}\,4} = \omega_I \approx \omega_{ci}\, \frac{N_{0p} m_p + N_{0i} m_i}{N_{0e} m_p} = \omega_{ci}(1 - \nu Z + \nu M) \tag{3.5}$$

(see e.g. Isenberg and Hollweg 1982; Isenberg 1984; Melrose 1986). Here the inequalities $\omega_{pe}^2 \gg \omega_{ce}^2$ and $m_e \ll m_p, m_i$ have been assumed. The condition $\omega_{pe}^2 \gg \omega_{ce}^2$ is well satisfied in most space plasmas.

Now, we only consider the wave properties of a plasma at rest, i.e. $v_{0\alpha} = 0$. In this case, we cannot distinguish waves that propagate parallel or antiparallel to the x axis. Therefore the polynomial (3.1) contains only even powers of k, and Q is an even number. The same arguments also apply to ω and P. Because of this symmetry,

https://doi.org/10.1017/S0022377897005758 Published online by Cambridge University Press

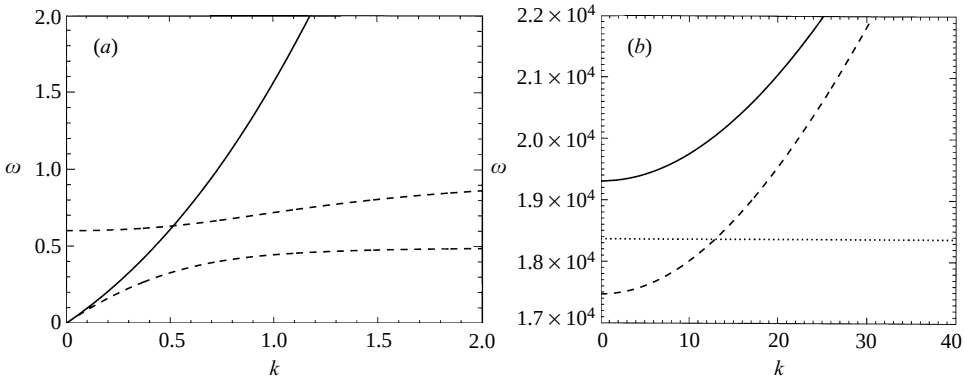


Figure 1. Normalized dispersion relations for wave propagation parallel to the ambient magnetic field in a cold plasma at rest. The plasma consists of 10% helium ions (doubly ionized), 90% protons and electrons. The electron plasma frequency ω_{pe} is ten times the electron gyrotron frequency ω_{ce}. Solid curves represent right-hand polarization, dashed curve left-hand polarization and dotted curves longitudinal polarization. (*a*) represents low-frequency modes and (*b*) high-frequency modes. The whistler mode (solid curve in (*a*)) ends at $\omega_{ce} = 1836$, which is not shown.

we consider only solutions with positive ω and k. Then, if our polynomial is of order P in ω, we shall find $\frac{1}{2}P$ different modes.

We now consider the dispersion relation of the cold plasma. The properties of a warm plasma will be investigated later.

First we investigate propagation parallel to the magnetic field, i.e. $\theta = 0$ (see Fig. 1). In this special case the evaluation of the dispersion relation can be done analytically. Then (2.13) results in

$$\epsilon_1(n^2 - \epsilon_2 + \epsilon_4)(n^2 - \epsilon_2 - \epsilon_4) = 0. \tag{3.6}$$

The first factor in (3.6) represents purely longitudinal waves at a fixed frequency, namely the plasma frequency ω_p. These waves are independent of k and are fully longitudinally polarized, i.e. $\xi = 1$. These are the so-called *Langmuir waves* (see Krall and Trivelpiece 1973).

The second factor in (3.6) leads to right-hand circularly polarized waves, i.e. $\sigma = 1$ and $\xi = 0$. The dispersion relation is given implicitly by

$$c^2k^2 - \omega^2 + \sum_\alpha \frac{\omega_{p\alpha}^2 \omega}{\omega + \omega_{c\alpha}} = 0, \tag{3.7}$$

leading to two different modes. One of them (see the solid curve in Fig. 1*b*) starts ($k = 0$) at ω_R with a horizontal tangent ($v_g = 0$) and ends as an electromagnetic wave with $v_g = c$ (see Krall and Trivelpiece 1973). The other mode (see the solid curve in Fig. 1*a*), starts at $\omega = 0$ with a group velocity

$$\begin{aligned} v_g^2 &= \frac{c^2}{1 + \omega_{pe}^2/\omega_{ce}^2 + \omega_{pp}^2/\omega_{cp}^2 + \omega_{pi}^2/\omega_{ci}^2} = v_A^2 \\ &\approx v_{\text{ref}}^2 \frac{N_0 m_p}{N_{0p} m_p + N_{0i} m_i} = \frac{B_0^2}{4\pi(N_{0p} m_p + N_{0i} m_i)}. \end{aligned} \tag{3.8}$$

This velocity is equal to the Alfvén speed v_A in the bi-ion plasma (v_{ref} is the Alfvén velocity of a pure electron–proton plasma). For increasing k, ω rises quickly and

https://doi.org/10.1017/S0022377897005758 Published online by Cambridge University Press

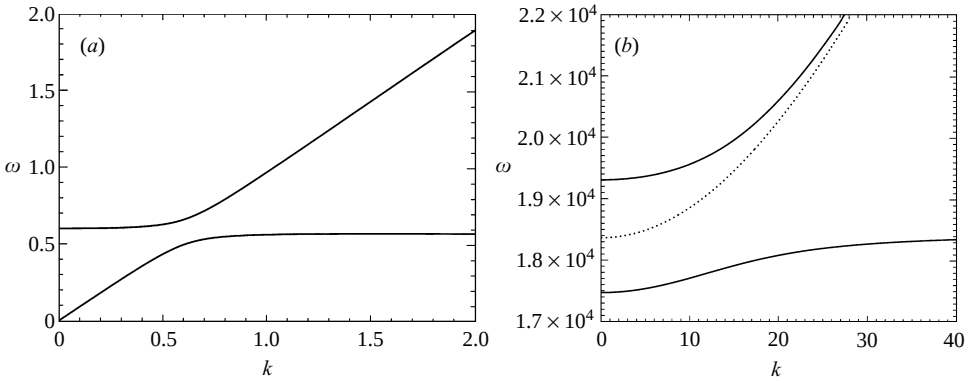


Figure 2. Normalized dispersion relations for wave propagation perpendicular to the ambient magnetic field in a cold plasma at rest. For a detailed description of the plasma parameters see Fig. 1. Solid curves represent extraordinary waves and dotted curves ordinary waves. (*a*) represents low-frequency modes and (*b*) high-frequency modes. The topmost extraordinary mode in (*a*) ends at $\omega_{LH} \approx 40$, which is not shown.

then tends asymptotically to ω_{ce}. This mode is the so-called *whistler mode* (see Krall and Trivelpiece 1973).

The third factor in (3.6) leads to left-hand circularly polarized waves, i.e. $\sigma = -1$ and $\xi = 0$. The dispersion relation is given implicitly by

$$c^2k^2 - \omega^2 + \sum_{\alpha} \frac{\omega_{p\alpha}^2 \omega}{\omega - \omega_{c\alpha}} = 0, \tag{3.9}$$

resulting in three different modes. One of them starts ($k = 0$) horizontally ($v_g = 0$) at ω_L and ends ($k \to \infty$) as an electromagnetic wave with $v_g = c$ (see the dashed curve in Fig. 1*b*). The second mode starts at ω_I with a horizontal tangent ($v_g = 0$) and ends asymptotically ($k \to \infty$) at ω_{cp} (see the dashed curve in Fig. 1*a*). The third mode starts at $\omega = 0$ with a group velocity that is also equal to the Alfvén velocity v_A. This mode goes asymptotically up to ω_{ci} for large k. Note that $\omega_{ci} < \omega_I < \omega_{cp}$. In a pure electron–proton plasma the last two modes would reduce to one mode (left-hand circularly polarized) going from $\omega = 0$ at $k = 0$ up to ω_{cp} for large k. Thus these two modes appear only in a bi-ion plasma. In Fig. 1 the dispersion relations are illustrated for a heavy ion component, with $\nu = 0.1$, $Z = 2$ and $M = 4$ (10% doubly ionized helium). Then ω_I takes the value of $0.6\,\omega_{cp}$ (see Fig. 1*a*).

Next we investigate propagation perpendicular to the magnetic field, i.e. for $\theta = \frac{1}{2}\pi$ (see Fig. 2). Evaluation of the determinant in (2.13) gives

$$(\epsilon_3 - n^2)[\epsilon_1 (\epsilon_2 - n^2) - \epsilon_6^2] = 0\ . \tag{3.10}$$

The first factor in (3.10) leads immediately to

$$\omega(k) = (\omega_p^2 + c^2k^2)^{1/2}\ . \tag{3.11}$$

This dispersion relation starts horizontally at ω_p represents an electromagnetic wave at higher wavenumbers k (see the dotted curve in Fig. 2*b*). The waves associated with this dispersion relation are polarized parallel to the ambient magnetic field, in the direction of $\mathbf{e}_z$, i.e. $\sigma = 0$ and $\xi = 0$. These waves are the so-called *ordinary waves* (see Krall and Trivelpiece 1973).

https://doi.org/10.1017/S0022377897005758 Published online by Cambridge University Press

The second factor in (3.10) can be written in the form

$$n^2 = \frac{(\omega_R^2 - \omega^2)(\omega_L^2 - \omega^2)(\omega_I^2 - \omega^2)}{(\omega_{UH}^2 - \omega^2)(\omega_{LH}^2 - \omega^2)(\omega_{IH}^2 - \omega^2)} \,. \tag{3.12}$$

The frequencies ω_{UH}, ω_{LH} and ω_{IH} are the positive roots of a polynomial of order 6 in ω. It contains only even powers of ω. These roots are found to be

$$\omega_{UH}^2 \approx \omega_{pe}^2 + \omega_{ce}^2 \,, \tag{3.13}$$

$$\omega_{LH}^2 \approx \frac{\omega_{ce}^2\,(\omega_{cp}^2 + \omega_{ci}^2 + \omega_{pp}^2 + \omega_{pi}^2)}{\omega_{pe}^2 + \omega_{ce}^2} \,, \tag{3.14}$$

$$\omega_{IH}^2 \approx \frac{\omega_{cp}^2\omega_{ci}^2 + \omega_{ci}^2\omega_{pp}^2 + \omega_{cp}^2\omega_{pi}^2}{\omega_{cp}^2 + \omega_{ci}^2 + \omega_{pp}^2 + \omega_{pi}^2} \tag{3.15}$$

when $v_{\rm A} \ll c$. Note that $\omega_{IH} < \omega_I < \omega_{LH} < \omega_L < \omega_{UH} < \omega_R$. In the special case $\omega_{pe}^2 \gg \omega_{ce}^2$, which is satisfied in most space plasmas, ω_{LH}^2 and ω_{IH}^2 reduce to

$$\omega_{LH}^2 = \frac{\omega_{ce}^2}{w_{pe}^2}\,(\omega_{pp}^2 + \omega_{pi}^2) = \omega_{cp}^2\,\frac{m_p}{m_e}\left(1 - \nu Z + \frac{\nu Z^2}{M}\right) \,, \tag{3.16}$$

$$\omega_{IH}^2 = \frac{\omega_{pp}^2\omega_{ci}^2 + \omega_{pi}^2\omega_{cp}^2}{\omega_{pp}^2 + \omega_{pi}^2} = \omega_{cp}^2\,\frac{(1-\nu Z)Z^2/M^2 + \nu Z^2/M}{1 - \nu Z + \nu Z^2/M} \,. \tag{3.17}$$

A plasma with a heavy ion component of $\nu = 0.1$, $Z = 2$ and $M = 4$ (10% doubly ionized helium) has $\omega_{LH} = 40.45\,\omega_{cp}$ and $\omega_{IH} = 0.577\,\omega_{cp}$ (see Fig. 2*a*).

Inspection of (3.12) reveals four different modes. We begin our discussion at low frequencies. The first mode starts at $\omega = 0$ with a group velocity $v_g = v_{\rm A}$, and tends asymptotically to ω_{IH} as $k \to \infty$ (see Melrose (1986); and the bottom curve in Fig. 2*a*). The second mode starts at ω_I with a horizontal tangent and ends ($k \to \infty$) at ω_{LH} (see the top curve in Fig. 2*a*). The third mode is similar to the second mode, but with frequencies ω_L and ω_{UH} (see the bottom curve in Fig. 2*b*). The fourth mode also starts horizontally at ω_R, and subsequently transforms to a wave with the speed of light (see Krall and Trivelpiece (1973) and the top curve in Fig. 2*b*). These so-called *extraordinary waves* are polarized in the (x, y) plane, i.e. there are simultaneously longitudinal and transverse electric fields with a phase shift of 90°.

Evaluation of the dispersion relations (2.13) for a cold bi-ion plasma shows that the heavy ion component strongly influences the low-frequency waves, i.e. at frequencies well below ω_{LH}, where new wave modes appear in addition to the modes existing in a pure electron–proton plasma. On the other hand, the high-frequency waves, i.e. at frequencies above ω_{LH}, are only influenced by heavy ions in a minor way.

In the oblique case the determinant in (2.13) does not factorize. Therefore the dispersion relation is given implicitly by a polynomial of order 12 in ω and of order 4 in k. The dispersion relation $\omega(k)$, the group velocity $v_g(k)$, the angle $\psi(k)$ between the direction of the group velocity and the ambient magnetic field, the helicity $\sigma(k)$, and the electrostatic part $\xi(k)$ of the oblique modes ($\theta = \frac{1}{6}\pi$) are plotted in Fig. 3.

In this case the wave modes circularly polarized in the case of parallel propagation are able to couple via the longitudinal electric field. Because of the geometry of oblique propagation, the longitudinal part ξ of the former purely circularly polarized modes is given roughly by $\sin\theta$.

https://doi.org/10.1017/S0022377897005758 Published online by Cambridge University Press

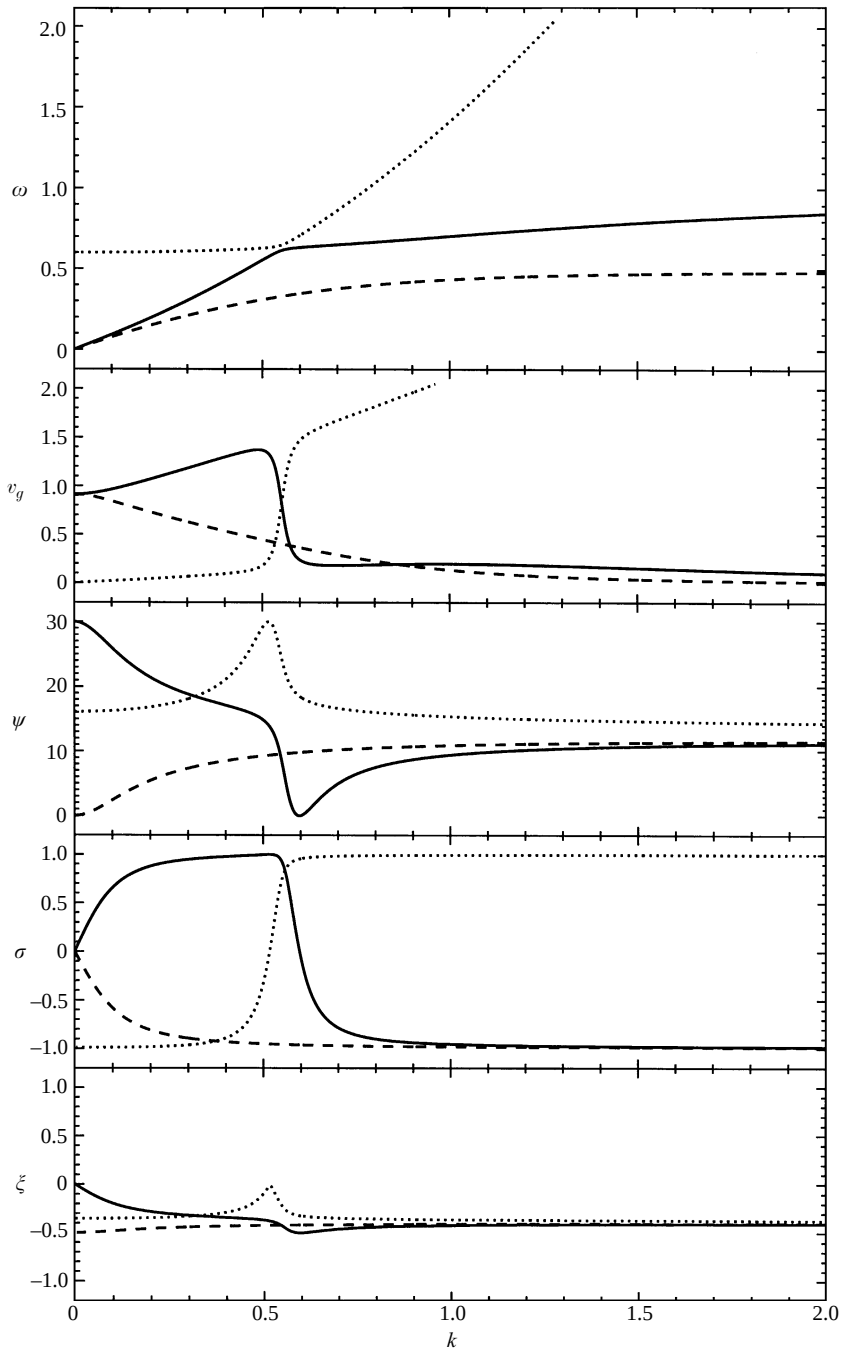


Figure 3. Normalized dispersion relations with group velocity v_g and polarization for oblique propagation at an angle of 30° to the ambient magnetic field in a cold plasma at rest. The direction ψ of the goup velocity is also measured from the ambient magnetic field. For a detailed description of the plasma parameters see Fig. 1. Each mode is represented by a different style of curve. The dotted dispersion relations ends at $\omega \approx 1588$, which is not shown. Note that the kink in ξ (dotted curve) at $k \approx 0.5$ is caused by a zero-crossing of the z component of the electric field amplitude (see 2.19)).

https://doi.org/10.1017/S0022377897005758 Published online by Cambridge University Press

At parallel propagation in the very low-frequency regime, the left- and right-hand circularly polarized waves propagate with the same speed, the Alfvén speed. These two circularly polarized waves can be regarded as being composed of two linearly polarized waves. In the case of propagation oblique to the ambient magnetic field, their phase velocities become different. Consequently, they are only linearly polarized (see Fig. 3), as is well known from magnetohydrodynamics, which is valid for $\omega \ll \omega_{ci}, \omega_{cp}$ (see Priest 1982).

In the oblique case (see Fig. 3) the wave modes starting at $\omega = 0$ and $k = 0$ are initially linearly polarized, as expected according to magnetohydrodynamics, i.e. they correspond to the *fast mode* and the *Alfvén mode*. Subsequently, they become elliptically polarized with increasing k. For large k the former Alfvén mode is transformed to a completely left-hand circularly polarized wave, and reaches ω_{ci} with a decreasing group velocity (see the dashed curves in Fig. 3). Initially, the other mode becomes right-hand polarized. Then it rapidly changes its polarization to a left-hand one, accompanied with a decreasing group velocity. For large k it becomes a purely left-hand circularly polarized wave (see the solid curves in Fig. 3). The third mode starts at ω_I at $k = 0$ and is initially left-hand polarized. Owing to mode coupling, it rapidly changes its sense of polarization near $k = 0.5$, accompanied with a strong jump in the group velocity. For large k this mode becomes a completely right-hand circularly polarized wave (see the dotted curves in Fig. 3). The electrostatic component of the individual waves is depicted in the bottom panel of Fig. 3.

In warm plasmas the determinant in (2.13) factorizes only in the parallel case in the same manner as shown in (3.6). But only the first factor, namely ϵ_1, differs from the cold case. Thus all new or different modes are longitudinally polarized. In the high-frequency regime the Langmuir waves behave like

$$\omega = \omega_{pe} + \frac{C_{se}^2}{2\omega_p^3}\, k^2 + O(k^4) \tag{3.18}$$

for small k. In the low-frequency regime two new modes with dispersion relations

$$\omega = v_{ph\pm} k + O(k^3) \tag{3.19}$$

emerge, with phase velocities

$$v_{ph\pm}^2 = \frac{1}{2}\left(C_{sp}^2 + C_{si}^2 + C_{se}^2\,\frac{\omega_{pp}^2 + \omega_{pi}^2}{\omega_{pe}^2}\right) \pm \frac{1}{2}\left[\left(C_{sp}^2 + C_{si}^2 + C_{se}^2\,\frac{\omega_{pp}^2 + \omega_{pi}^2}{\omega_{pe}^2}\right)^2 - 4\left(C_{sp}^2 C_{si}^2 + \frac{\omega_{pp}^2}{\omega_{pe}^2}\, C_{se}^2 C_{si}^2 + \frac{\omega_{pi}^2}{\omega_{pe}^2}\, C_{se}^2 C_{sp}^2\right)\right]^{1/2}. \tag{3.20}$$

If the heavy ion component is regarded as a minor component, i.e. $\nu \ll 1$, these phase velocities reduce to

$$v_{ph+}^2 = \frac{\gamma_p k_B T_p + \gamma_e k_B T_e}{m_p}, \tag{3.21}$$

$$v_{ph-}^2 = \frac{\gamma_i k_B T_i}{m_i}. \tag{3.22}$$

This result agrees with that previously derived by McKenzie *et al.* (1993). The additional appearance of two acoustic modes is demonstrated in Fig. 4(*a*) for parallel

https://doi.org/10.1017/S0022377897005758 Published online by Cambridge University Press

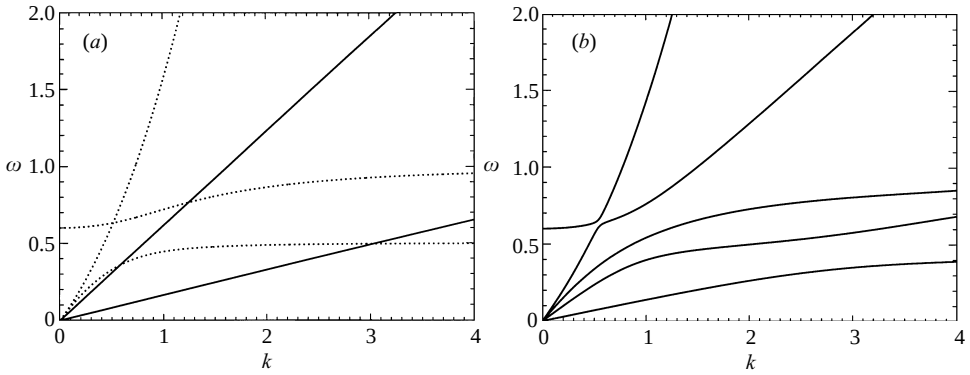


Figure 4. Normalized dispersion relations for propagation parallel and oblique ($\theta = 30^\circ$ to the ambient magnetic field in a warm plasma at rest. For a detailed description of the plasma parameters see Fig. 1. In this warm case the plasma parameters are supplemented by the plasma betas of the three components: $\beta_e = 0.4$, $\beta_p = 0.08$ and $\beta_i = 0.01$. (*a*) represents parallel propagation and (*b*) oblique propagation. In (*a*) figure additional modes with respect to the cold plasma are shown by solid curves, while the modes also existing in the cold plasma are shown by dotted curves. In (*b*) all warm modes are shown by solid curves.

propagation in a warm plasma with $T_e = 4T_p = 4T_i$, i.e., $\beta_e = 0.4$, $\beta_p = 0.08$ and $\beta_i = 0.01$. All other parameters are chosen as before.

For oblique propagation the dispersion relation is given implicitly by a polynomial of order 16 in ω and of order 10 in k. Therefore an analytic examination without rather drastic assumptions is not tractable. As in the cold case, the five different modes couple via the longitudinal electric field (see Fig. 4*b*).

The polarization properties of the warm modes presented in Fig. 4(*b*) are depicted in Fig. 5. There are five different modes. The plasma betas are chosen as $\beta_e = 0.4$, $\beta_p = 0.08$ and $\beta_i = 0.01$, i.e. $T_e = 4T_p = 4T_i$. Now these five modes couple with each other.

The wave mode (dotted curves) starting at ω_I and $k = 0$ is initially left-hand circularly polarized, and transforms into a right-hand circularly polarized mode near $k = 0.5$. This mode is weakly electrostatic, i.e. $|\xi| < 0.4$.

The mode depicted by the solid curves in Fig. 5 is initially linearly polarized and becomes right-hand elliptically polarized with increasing k. Near $k = 0.5$ its sense of polarization changes rapidly from right- to left-handed. Asymptotically, it is linearly polarized and mainly electrostatic for large k.

The third mode (see the dashed curves in Fig. 5) is also initially linearly polarized, and becomes left-hand elliptically polarized. Subsequently the ellipse degenerates to linear polarization in the (x, z) plane, i.e. $E_y = 0$ at $k \approx 0.9$. At this point the mode is already mainly electrostatic polarized, and remains is for increasing wavenumbers k. Between $k \approx 0.8$ and $k \approx 1.15$, the mode is right-hand elliptically polarized. At $k \approx 1.15$ the sense of polarization changes from right- to left-handed through $E_z = 0$. Therefore there is a discontinuity in ξ (see (2.19)).

The other two modes (see the two sorts of dot–dashed curves in Fig. 5) are initially linearly polarized, and become left-hand circularly polarized for large k, where they reach the frequencies ω_{ci} and ω_{cp} for large k. In this region they are mainly

https://doi.org/10.1017/S0022377897005758 Published online by Cambridge University Press

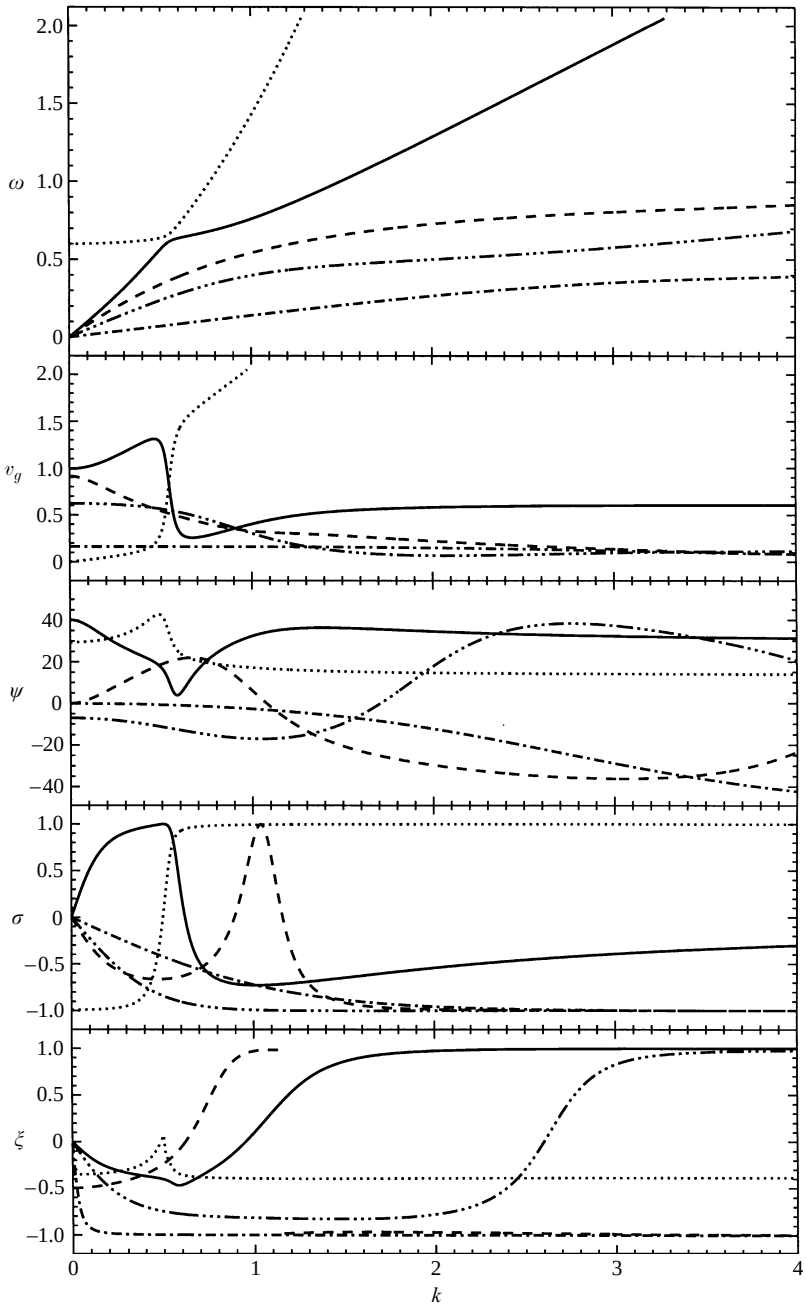


Figure 5. Normalized dispersion relations, group velocity v_g and polarization for oblique propagation at an angle of 30° to the ambient magnetic field in a warm plasma at rest. The direction ψ of the group velocity is also measured from the ambient magnetic field. For a description of the plasma parameters see Fig. 1. In this warm case the plasma parameter set is supplemented by the plasma betas of the three components: $\beta_e = 0.4$, $\beta_p = 0.08$ and $\beta_i = 0.01$. Each mode is shown by a different style of curve. Note that the discontinuities of ξ at $k \approx 0.0502$ (dotted curves) and at $k \approx 1.16$ (dashed curves) are caused by a zero-crossing of the z component of the electric field amplitude (see (2.19)).

https://doi.org/10.1017/S0022377897005758 Published online by Cambridge University Press

electrostatic, i.e. $|\xi| \to 1$. Thus Fig. 5 illustrates impressively the way in which the polarization properties of these modes depend on the minor ions in a warm plasma.

On comparing Figs 3 and 5, it is evident that the finite β_α strongly influence the properties of dispersion and polarization, especially in the region of large k, i.e. $k \to \infty$.

However, we should emphasize that strong thermal ion cyclotron damping appears if the wavelength λ is of the same order of magnitude as the gyroradius r_{Li} of the ions, i.e. $\lambda \approx r_{Li} = 2\pi v_{\mathrm{th}_i}/\omega_{ci}$ (see Krall and Trivelpiece 1987). According to the normalization employed in this paper, thermal ion cyclotron damping becomes important for wavenumbers $k^2 \approx 2\nu Z^2/M\beta_i = 2(Z^2/M)\beta_e^{-1}(T_e/T_i)$. This estimate also holds for protons ($Z = 1$, $M = 1$, $T_i = T_p$). Thus this wave-mode analysis is only valid in the range of wavenumbers determined by

$$k^2 \ll 2\frac{Z^2}{M}\frac{1}{\beta_e}\frac{T_e}{T_i}. \tag{3.23}$$

In the special case $Z = 2$, $M = 4$, $\beta_e = 0.4$, $T_e = 4T_i$ and $T_i = T_p$ this requirement leads to $k \ll 4.5$.

4. Discussion

In this paper we have extensively discussed the properties of plasma waves in a multicomponent plasma, especially a bi-ion plasma, by employing the multi-fluid plasma equations. The properties of pure electron–proton plasmas and multi-ion plasmas differ mainly in the low-frequency regime $\omega \ll \omega_{LH}$. As initially expected, the high-frequency plasma waves are dominated by electron dynamics. Therefore only slight differences can be found for $\omega \gg \omega_{LH}$. Thus we have restricted ourselves to low frequencies.

Each additional ion component produces a new cut-off frequency at $k = 0$ and a new resonance frequency at $k \to \infty$, and is accompanied by the appearance of a new mode. In the case of propagation oblique to the ambient magnetic field, this newly emerging mode couples with the others owing to the action of the longitudinal electric field. This mode coupling may lead to a change in the sense of polarization within an individual mode, e.g. a change from right- to left-hand polarization, as well as to a change from an elliptically polarized wave to a purely longitudinal wave, as illustrated in Figs 3–5.

Thus the minor heavy ion component essentially influences the dispersion and polarization of plasma waves, particularly in the low-frequency regime. Such minor-ion-related waves are observed through their magnetic field fluctuations in space plasmas. Our present results will contribute to the diagnostics of observed waves and the understanding of the properties of the magnetic field fluctuations found from extraterrestrial *in situ* measurements.

Acknowledgements

The authors are indebted to J. F. McKenzie, F. Verheest and U. Motschmann for useful discussions. The authors thank the Deutsche Forschungsgemeinschaft for supporting this work under Grant Ma 1376/6-1.

https://doi.org/10.1017/S0022377897005758 Published online by Cambridge University Press

Appendix

Here the basic equations introduced in Sec. 2 are treated in greater detail, i.e. with regard to normalization, linearization and Fourier transformation.

The time is normalized to the inverse proton cyclotron frequency $\omega_{cp} = eB_0/m_pc$, and the spatial coordinates are given in terms of the reference length $l_{\rm ref} = (m_pc^2/4\pi N_{0e}e^2)^{1/2}$. Then, the reference velocity is found to be $v_{\rm ref} = l_{\rm ref}\omega_{cp} = B_0/(4\pi m_pN_{0e})^{1/2}$. The speed $v_{\rm ref}$ corresponds to the Alfvén velocity in a pure electron–proton plasma with particle number densities equal to N_{0e}. Note that this normalization is independent of the ion composition of the plasma. Furthermore, the magnetic field, the particle number densities and all velocities are normalized by the undisturbed background magnetic field $B_{\rm ref} = B_0$, the unperturbed particle number densities $N_{{\rm ref}\alpha} = N_{0\alpha}$ and the reference velocity $v_{\rm ref}$ respectively. Unnormalized quantities will be indicated by a prime ($'$) if they could be confused with the normalized ones. After this straightforward normalization, linearization of (2.1)–(2.9) (disturbances of quadratic and higher order are neglected) provides the following equations:

$$\frac{\partial}{\partial t} N_\alpha + \nabla \cdot \mathbf{v}_\alpha + v_{0\alpha}\mathbf{e}_B \nabla N_\alpha = 0, \tag{A 1}$$

$$\frac{\partial}{\partial t} \mathbf{v}_\alpha + (v_{0\alpha}\mathbf{e}_B \cdot \nabla)\mathbf{v}_\alpha + C_{s\alpha}^2 \nabla N_\alpha - \omega_{c\alpha}(\mathbf{E} + v_{0\alpha}\mathbf{e}_B \times \mathbf{B} + \mathbf{v}_\alpha \times \mathbf{e}_B) = 0, \tag{A 2}$$

$$\nabla \times \mathbf{E} = -\frac{\partial}{\partial t}\mathbf{B}, \tag{A 3}$$

$$\nabla \times \mathbf{B} = \frac{1}{c^2}\frac{\partial}{\partial t}\mathbf{E} + \frac{1}{c^2}\mathbf{j}, \tag{A 4}$$

$$\nabla \cdot \mathbf{E} = \rho, \tag{A 5}$$

$$\nabla \cdot \mathbf{B} = 0, \tag{A 6}$$

$$\rho = \sum_\alpha \frac{\omega_{p\alpha}^2}{\omega_{c\alpha}} N_\alpha, \tag{A 7}$$

$$\mathbf{j} = \sum_\alpha \frac{\omega_{p\alpha}^2}{\omega_{c\alpha}} (\mathbf{v}_\alpha + v_{0\alpha}\mathbf{e}_B N_\alpha), \tag{A 8}$$

with

$$C_{s\alpha}^2 = \frac{C_{s\alpha}'^2}{v_{\rm ref}^2} = \frac{\gamma_\alpha\beta_\alpha}{2}\frac{N_0}{N_{0\alpha}}\frac{m_p}{m_\alpha}, \tag{A 9}$$

$$\omega_{c\alpha} = \frac{\omega_{c\alpha}'}{\omega_{cp}'} = \frac{q_\alpha}{e}\frac{m_p}{m_\alpha}, \tag{A 10}$$

$$\omega_{p\alpha}^2 = \frac{\omega_{p\alpha}'^2}{\omega_{cp}'^2}\frac{q_\alpha^2}{e^2}\frac{m_p}{m_\alpha}\frac{4\pi N_0 m_p c^2}{B_0^2}. \tag{A 11}$$

The plasma beta of each component is given by $\beta_\alpha = 8\pi N_{0\alpha}k_BT_\alpha/B_0^2$ (where T_α is the temperature of the particle component α). Furthermore, $C_{s\alpha}' = (\gamma_\alpha k_BT_\alpha/m_\alpha)^{1/2}$ represents the sound speed of each component, $\omega_{c\alpha}' = q_\alpha B_0/m_\alpha c$ and $\omega_{p\alpha}' = (4\pi q_\alpha^2 N_{0\alpha}/m_\alpha)^{1/2}$ denote the cyclotron frequency and the plasma frequency of each component respectively.

https://doi.org/10.1017/S0022377897005758 Published online by Cambridge University Press

Note that N_α, $\mathbf{v}_\alpha$, $\mathbf{E}$, $\mathbf{B}$, $\mathbf{j}$ and ρ now describe the perturbations and are zero in the undisturbed (background) state. $v_{0\alpha}$ and c are also normalized in the aforementioned manner. Note also that the cyclotron frequency $\omega_{c\alpha}$ is negative for electrons. However, despite this, we shall denote ω_{ce} as a positive quantity. Therefore the sign has to be changed after substituting $\omega_{c\alpha}$ by ω_{ce}.

Consequently, the requirement of charge neutrality and current-free state in the undisturbed case can be written in dimensionless form as

$$\sum_\alpha \frac{\omega_{p\alpha}^2}{\omega_{c\alpha}} = 0, \tag{A 12}$$

$$\sum_\alpha \frac{\omega_{p\alpha}^2}{\omega_{c\alpha}} v_{0\alpha} = 0 \tag{A 13}$$

respectively.

This set of coupled linear differential equations (A 1)–(A 8) is now transformed to a set of algebraic equations by Fourier transformation, i.e. we assume that N_α, $\mathbf{v}_\alpha$, $\mathbf{E}$, $\mathbf{B} \propto \exp[i\,(\mathbf{k}\cdot\mathbf{x} - \omega t)]$:

$$(v_{0\alpha}\mathbf{e}_B \cdot \mathbf{k} - \omega)N_\alpha + \mathbf{k}\cdot\mathbf{v}_\alpha = 0, \tag{A 14}$$

$$(v_{0\alpha}\mathbf{e}_B \cdot \mathbf{k} - \omega)\mathbf{v}_\alpha + C_{s\alpha}^2 \mathbf{k} N_\alpha + i\omega_{c\alpha}\,(\mathbf{E} + v_{0\alpha}\mathbf{e}_B \times \mathbf{B} + \mathbf{v}_\alpha \times \mathbf{e}_B) = 0, \tag{A 15}$$

$$i\mathbf{k}\times\mathbf{E} = i\omega\mathbf{B}, \tag{A 16}$$

$$i\mathbf{k}\times\mathbf{B} = \frac{-i\omega}{c^2}\mathbf{E} + \frac{1}{c^2}\,\mathbf{j}, \tag{A 17}$$

$$i\mathbf{k}\cdot\mathbf{E} = \rho, \tag{A 18}$$

$$i\mathbf{k}\cdot\mathbf{B} = 0. \tag{A 19}$$

Since we are interested in the study of plane waves, the wave vector is assumed to be directed along the x axis, i.e. $\mathbf{k} = k\,\mathbf{e}_x$, and the ambient magnetic field lies in the (x, z) plane, i.e. $\mathbf{e}_B = \cos\theta\,\mathbf{e}_x + \sin\theta\,\mathbf{e}_z$. The particle number density N_α and the magnetic field $\mathbf{B}$ in (A 15) are eliminated by employing (A 14) and (A 16). Then the resulting system of equations depends only on $\mathbf{v}_\alpha$ and $\mathbf{E}$, and thus can be written in matrix form as

$$\mathscr{L}_\alpha \cdot \mathbf{v}_\alpha + \mathscr{M}_\alpha \cdot \mathbf{E} = 0\ . \tag{A 20}$$

The matrices $\mathscr{L}_\alpha$ and $\mathscr{M}_\alpha$ are given by

$$\mathscr{L}_\alpha = (v_{0\alpha}\mathbf{e}_B\cdot\mathbf{k} - \omega)\mathbf{1} - \frac{C_{s\alpha}^2}{v_{0\alpha}\mathbf{e}_B\cdot\mathbf{k} - w}\,\mathbf{k}\otimes\mathbf{k} - i\omega_{c\alpha}\,\mathbf{e}_B\times\mathbf{1}, \tag{A 21}$$

$$\mathscr{M}_\alpha = \frac{i\omega_{c\alpha}v_{0\alpha}k}{\omega}\,(\mathbf{e}_B\times\mathbf{1})\cdot(\mathbf{e}_x\times\mathbf{1}) + i\omega_{c\alpha}\,\mathbf{1}\ . \tag{A 22}$$

Here $\cdot$, $\times$ and $\otimes$ denote the scalar, cross and dyadic products respectively, and $\mathbf{1}$ is the unit matrix. Equation (A 20) represents an inhomogeneous system of equations for each component. Its solution is obtained by matrix inversion, and has the form

$$\mathbf{v}_\alpha = -\mathscr{L}_\alpha^{-1}\cdot\mathscr{M}_\alpha\cdot\mathbf{E}\ . \tag{A 23}$$

https://doi.org/10.1017/S0022377897005758 Published online by Cambridge University Press

The tensor or matrix $\mathscr{L}_\alpha^{-1} \cdot \mathscr{M}_\alpha$ may be considered as a mobility tensor. If the current is expressed by

$$\mathbf{j} = \sum_\alpha \mathscr{K}_\alpha \cdot \mathbf{v}_\alpha, \tag{A 24}$$

with

$$\mathscr{K}_\alpha = \frac{\omega_{c\alpha} c^2}{v_{\mathrm{A}\alpha}^2}\,\mathbf{1} - \frac{\omega_{c\alpha} c^2 v_{0\alpha}}{v_{\mathrm{A}\alpha}^2 (v_{0\alpha}\mathbf{e}_B \cdot \mathbf{k} - \omega)}\,\mathbf{e}_B \otimes \mathbf{k}, \tag{A 25}$$

then the conductivity tensor $\boldsymbol{\sigma}$ defined by $\mathbf{j} = \boldsymbol{\sigma} \cdot \mathbf{E}$ is found to be

$$\boldsymbol{\sigma} = -\sum_\alpha \mathscr{K}_\alpha \mathscr{L}_\alpha^{-1} \mathscr{M}_\alpha\ . \tag{A 26}$$

The wave equation for $\mathbf{E}$ is now derived by calculating $\boldsymbol{\nabla} \times (\boldsymbol{\nabla} \times \mathbf{E})$ or $\mathbf{k} \times (\mathbf{k} \times \mathbf{E})$, resulting in

$$[n^2\,(\mathbf{e}_x \otimes \mathbf{e}_x - \mathbf{1}) + \boldsymbol{\epsilon}]\,\mathbf{E} = 0 \tag{A 27}$$

(see e.g. Suchy 1996), with the refractive index $n = ck/\omega$ and the dielectric tensor $\boldsymbol{\epsilon} = \mathbf{1} + (i/\omega)\,\boldsymbol{\sigma}$. An explicit calculation of the dielectric tensor leads to

$$\boldsymbol{\epsilon} = \begin{pmatrix} \epsilon_1 & i\epsilon_6 & \epsilon_5 \\ -i\epsilon_6 & \epsilon_2 & i\epsilon_4 \\ \epsilon_5 & -i\epsilon_4 & \epsilon_3 \end{pmatrix}, \tag{A 28}$$

with

$$\epsilon_1 = 1 - \sum_\alpha \frac{\omega^2\,\omega_{p\alpha}^2}{\Delta_\alpha}\,[(\omega - v_{0\alpha}k\cos\theta)^2 - \omega_{c\alpha}^2\cos^2\theta]\ , \tag{A 29}$$

$$\epsilon_2 = 1 - \sum_\alpha \frac{\omega_{p\alpha}^2}{\Delta_\alpha}\,[(\omega - v_{0\alpha}k\cos\theta)^2 - C_{s\alpha}^2 k^2]\,(\omega - v_{0\alpha}k\cos\theta)^2\ , \tag{A 30}$$

$$\begin{aligned}\epsilon_3 = 1 - \sum_\alpha \frac{\omega_{p\alpha}^2}{\Delta_\alpha}\,&[(\omega^2 - 2\,\omega\,v_{0\alpha}k\cos\theta + {v_{0\alpha}}^2k^2 - C_{s\alpha}^2k^2)\,(\omega - v_{0\alpha}k\cos\theta)^2 \\ &-\omega^2\,\omega_{c\alpha}^2\sin^2\theta]\ ,\end{aligned} \tag{A 31}$$

$$\begin{aligned}\epsilon_4 = -\sum_\alpha \frac{\omega_{c\alpha}\omega_{p\alpha}^2}{\Delta_\alpha}\,&[(\omega^2 - 2\,\omega\,v_{0\alpha}k\cos\theta + {v_{0\alpha}}^2k^2 - C_{s\alpha}^2k^2)\cos\theta \\ &-\omega\,v_{0\alpha}k\sin^2\theta]\,(\omega - v_{0\alpha}k\cos\theta)\ ,\end{aligned} \tag{A 32}$$

$$\epsilon_5 = -\sum_\alpha \frac{\omega\,\omega_{p\alpha}^2\sin\theta}{\Delta_\alpha}\,[v_{0\alpha}k\,(\omega - v_{0\alpha}k\cos\theta)^2 - \omega\,\omega_{c\alpha}^2\cos\theta]\ , \tag{A 33}$$

$$\epsilon_6 = -\sum_\alpha \frac{\omega\,\omega_{c\alpha}\omega_{p\alpha}^2\sin\theta}{\Delta_\alpha}\,(\omega - v_{0\alpha}k\cos\theta)^2\ , \tag{A 34}$$

$$\begin{aligned}\Delta_\alpha = \omega^2\,\{&[(\omega - v_{0\alpha}k\cos\theta)^2 - C_{s\alpha}^2k^2]\,(\omega - v_{0\alpha}k\cos\theta)^2 \\ &-\omega_{c\alpha}^2[(\omega - v_{0\alpha}k\cos\theta)^2 - C_{s\alpha}^2k^2\cos^2\theta]\}.\end{aligned} \tag{A 35}$$

Equation (A 27) is the starting point for the linear mode analysis presented in Sec. 3.

https://doi.org/10.1017/S0022377897005758 Published online by Cambridge University Press

References

Fairfield, D. H. and Behannon, K. W. 1976 *J. Geophys. Res.* **81**, 3897.

Gary, S. P. 1991 *Space Sci. Rev.* **56**, 373.

Goldstein, M. L., Smith, C. W. and Matthaeus, W. H. 1983 *J. Geophys. Res.* **81**, 9989.

Goldstein, M. L., Wong, H. K. and Glassmeier, K. H. 1990 *J. Geophys. Res.* **95**, 947.

Hamelin, M. and Beghin, C. 1976 *J. Plasma Phys.* **15**, 115.

Hizanidis, K., Cargill, P. J. and Papadopoulos, K. 1988 *J. Geophys. Res.* **93**, 9577.

Hoppe, M. M. and Russell, C. T. 1981 *Adv. Space Res.* **1**, 327.

Hoppe, M. M., Russell, C. T., Frank, L. A., Eastman, T. E. and Greenstadt, E. W. 1981 *J. Geophys. Res.* **86**, 4471.

Isenberg, P. A. 1984 *J. Geophys. Res.* **89**, 2133.

Isenberg, P. A. and Hollweg, J. V. 1982 *J. Geophys. Res.* **87**, 5023.

Krall N. A. and Trivelpiece A. W. 1973 *Principles of Plasma Physics*. McGraw-Hill, New York (reprinted 1986 by San Francisco Press).

Krauss-Varban, D., Omidi, N. and Quest, K. B. 1994 *J. Geophys. Res.* **99**, 5987.

McKenzie, J. F., Marsch, E., Baumgärtel, K. and Sauer, K. 1993 *Ann. Geophys.* **11**, 341.

Mann, G. and Lühr, H. 1991 *Ann. Geophys.* **9**, 681.

Marsch, E. 1991 *Physics of the Inner Heliosphere* (ed. R. Schwenn and E. Marsch), p. 45. Springer-Verlag, Berlin.

Melrose D. B. 1986 *Instabilities in Space and Laboratory Plasmas*. Cambridge University Press.

Miller, J. A. and Viñas, A. F. 1993 *Astrophys. J.* **412**, 386.

Oscarson, T. and Andre M. 1986 *Ann. Geophys.* **4**, 319.

Paschmann, G., Sckopke, N., Bame, S. J., Asbridge, J. R., Gosling, J. T., Russell, C. T. and Greenstadt, E. W. 1979 *Geophys. Res. Lett.* **6**, 209.

Priest, E. R. 1982 *Solar Magnetohydrodynamics* Kluwer, Dordrecht.

Riedler, W., Schwingenschuh, K., Yeroshenko, Ye. G., Styashkin, V. A. and Russell, C. T. 1986 *Nature* **321**, 288.

Rönnmark, K. 1982 *Kiruna Geophysical Institute Report* No. 179.

Smith, R. L. and Brice, N. 1964 *J. Geophys. Res.* **69**, 5029.

Suchy, K. 1996 *The Upper Atmosphere* (ed. W. Dieminger, G. K. Hartmann and R. Leitinger), p. 287, Springer-Verlag, Berlin.

Temerin, M. and Roth, I. 1992 *Astrophys. J. Lett.* **391**, L105

Thomsen, M. F. 1985 *Collisionless Shocks in the Heliosphere: Review of Current Research* (ed. B. T. Tsurutani and R. G. Stone), p. 253. Geophysical Monograph 35, AGU, Washington, DC.

Thomsen, M. F., Feldman, W. C., Wilken, B., Jockers, K., Stüdemann, W., Johnstone, A. D.,Coates, A., Formisano, V., Amata, E., Winningham, J. D., Borg, H., Bryant, D. and Wallis, M. K. 1987 *Astron. Astrophys.* **187**, 141.

Tsurutani, B. T. and Smith, E. J. 1986 *Geophys. Res. Lett.* **13**, 259.

Tsurutani, B. T., Thorne, R. M., Smith, E. J., Gosling, J. T. and Matsumoto, H. 1987*a* *J. Geophys. Res.* **92**, 11 074.

Tsurutani, B. T., Brinca, A. L., Smith, E. J., Thorne, R. M., Scarf, F. L., Gosling, J. T. and Ipavich, F. M. 1987*b* *Astron. Astrophys.* **187**, 97.

Verheest, F. 1977 *Astrophys. Space Sci.* **46**, 165.

Zank, G. P. and McKenzie, J. F. 1988 *J. Plasma Phys.* **39**, 183.

https://doi.org/10.1017/S0022377897005758 Published online by Cambridge University Press